First observation of the semileptonic decay $\Lambda_c^+ \to pK^- e^+ \nu_e$

M. Ablikim,[1] M. N. Achasov,[11,b] P. Adlarson,[70] M. Albrecht,[4] R. Aliberti,[31] A. Amoroso,[69a,69c] M. R. An,[35] Q. An,[66,53] X. H. Bai,[61] Y. Bai,[52] O. Bakina,[32] R. Baldini Ferroli,[26a] I. Balossino,[1,27a] Y. Ban,[42,g] V. Batozskaya,[1,40] D. Becker,[31] K. Begzsuren,[29] N. Berger,[31] M. Bertani,[26a] D. Bettoni,[27a] F. Bianchi,[69a,69c] J. Bloms,[63] A. Bortone,[69a,69c] I. Boyko,[32] R. A. Briere,[5] A. Brueggemann,[63] H. Cai,[71] X. Cai,[1,53] A. Calcaterra,[26a] G. F. Cao,[1,58] N. Cao,[1,58] S. A. Cetin,[57a] J. F. Chang,[1,53] W. L. Chang,[1,58] G. Chelkov,[32,a] C. Chen,[39] Chao Chen,[50] G. Chen,[1] H. S. Chen,[1,58] M. L. Chen,[1,53] S. J. Chen,[38] S. M. Chen,[56] T. Chen,[1] X. R. Chen,[28,58] X. T. Chen,[1] Y. B. Chen,[1,53] Z. J. Chen,[23,h] W. S. Cheng,[69c] S. K. Choi,[50] X. Chu,[39] G. Cibinetto,[27a] F. Cossio,[69c] J. J. Cui,[45] H. L. Dai,[1,53] J. P. Dai,[73] A. Dbeyssi,[17] R. E. de Boer,[4] D. Dedovich,[32] Z. Y. Deng,[1] A. Denig,[31] I. Denysenko,[32] M. Destefanis,[69a,69c] F. De Mori,[69a,69c] Y. Ding,[36] J. Dong,[1,53] L. Y. Dong,[1,58] M. Y. Dong,[1,53,58] X. Dong,[71] S. X. Du,[75] P. Egorov,[32,a] Y. L. Fan,[71] J. Fang,[1,53] S. S. Fang,[1,58] W. X. Fang,[1] Y. Fang,[1] R. Farinelli,[27a] L. Fava,[69b,69c] F. Feldbauer,[4] G. Felici,[26a] C. Q. Feng,[66,53] J. H. Feng,[54] K. Fischer,[64] M. Fritsch,[4] C. Fritzsch,[63] C. D. Fu,[1] H. Gao,[58] Y. N. Gao,[42,g] Yang Gao,[66,53] S. Garbolino,[69c] I. Garzia,[27a,27b] P. T. Ge,[71] Z. W. Ge,[38] C. Geng,[54] E. M. Gersabeck,[62] A. Gilman,[64] K. Goetzen,[12] L. Gong,[36] W. X. Gong,[1,53] W. Gradl,[31] M. Greco,[69a,69c] L. M. Gu,[38] M. H. Gu,[1,53] Y. T. Gu,[14] C. Y. Guan,[1,58] A. Q. Guo,[28,58] L. B. Guo,[37] R. P. Guo,[44] Y. P. Guo,[10,f] A. Guskov,[32,a] T. T. Han,[45] W. Y. Han,[35] X. Q. Hao,[18] F. A. Harris,[60] K. K. He,[50] K. L. He,[1,58] F. H. Heinsius,[4] C. H. Heinz,[31] Y. K. Heng,[1,53,58] C. Herold,[55] M. Himmelreich,[12,d] G. Y. Hou,[1,58] Y. R. Hou,[58] Z. L. Hou,[1] H. M. Hu,[1,58] J. F. Hu,[51,i] T. Hu,[1,53,58] Y. Hu,[1] G. S. Huang,[66,53] K. X. Huang,[54] L. Q. Huang,[67] L. Q. Huang,[28,58] X. T. Huang,[45] Y. P. Huang,[1] Z. Huang,[42,g] T. Hussain,[68] N. Hüsken,[25,31] W. Imoehl,[25] M. Irshad,[66,53] J. Jackson,[25] S. Jaeger,[4] S. Janchiv,[29] E. Jang,[50] J. H. Jeong,[50] Q. Ji,[1] Q. P. Ji,[18] X. B. Ji,[1,58] X. L. Ji,[1,53] Y. Y. Ji,[45] Z. K. Jia,[66,53] H. B. Jiang,[45] S. S. Jiang,[35] X. S. Jiang,[1,53,58] Y. Jiang,[58] J. B. Jiao,[45] Z. Jiao,[21] S. Jin,[38] Y. Jin,[61] M. Q. Jing,[1,58] T. Johansson,[70] N. Kalantar-Nayestanaki,[59] X. S. Kang,[36] R. Kappert,[59] M. Kavatsyuk,[59] B. C. Ke,[75] I. K. Keshk,[4] A. Khoukaz,[63] P. Kiese,[31] R. Kiuchi,[1] R. Kliemt,[12] L. Koch,[33] O. B. Kolcu,[57a] B. Kopf,[4] M. Kuemmel,[4] M. Kuessner,[4] A. Kupsc,[40,70] W. Kühn,[33] J. J. Lane,[62] J. S. Lange,[33] P. Larin,[17] A. Lavania,[24] L. Lavezzi,[69a,69c] Z. H. Lei,[66,53] H. Leithoff,[31] M. Lellmann,[31] T. Lenz,[31] C. Li,[43] C. Li,[39] C. H. Li,[35] Cheng Li,[66,53] D. M. Li,[75] F. Li,[1,53] G. Li,[1] H. Li,[47] H. Li,[66,53] H. B. Li,[1,58] H. J. Li,[18] H. N. Li,[51,i] J. Q. Li,[4] J. S. Li,[54] J. W. Li,[45] Ke Li,[1] L. J. Li,[1] L. K. Li,[1] Lei Li,[3,m] M. H. Li,[39] P. R. Li,[34,j,k] S. X. Li,[10] S. Y. Li,[56] T. Li,[45] W. D. Li,[1,58] W. G. Li,[1] X. H. Li,[66,53] X. L. Li,[45] Xiaoyu Li,[1,58] H. Liang,[66,53] H. Liang,[1,58] H. Liang,[30] Y. F. Liang,[49] Y. T. Liang,[28,58] G. R. Liao,[13] L. Z. Liao,[45] J. Libby,[24] A. Limphirat,[55] C. X. Lin,[54] D. X. Lin,[28,58] T. Lin,[1] B. J. Liu,[1] C. X. Liu,[1] D. Liu,[17,66] F. H. Liu,[48] Fang Liu,[1] Feng Liu,[6] G. M. Liu,[51,i] H. Liu,[34,j,k] H. B. Liu,[14] H. M. Liu,[1,58] Huanhuan Liu,[1] Huihui Liu,[19] J. B. Liu,[66,53] J. L. Liu,[67] J. Y. Liu,[1,58] K. Liu,[1] K. Y. Liu,[36] Ke Liu,[20] L. Liu,[66,53] M. H. Liu,[10,f] P. L. Liu,[1] Q. Liu,[58] S. B. Liu,[66,53] T. Liu,[10,f] W. K. Liu,[39] W. M. Liu,[66,53] X. Liu,[34,j,k] Y. Liu,[34,j,k] Y. B. Liu,[39] Z. A. Liu,[1,53,58] Z. Q. Liu,[45] X. C. Lou,[1,53,58] F. X. Lu,[54] H. J. Lu,[21] J. G. Lu,[1,53] X. L. Lu,[1] Y. Lu,[7] Y. P. Lu,[1,53] Z. H. Lu,[1] C. L. Luo,[37] M. X. Luo,[74] T. Luo,[10,f] X. L. Luo,[1,53] X. R. Lyu,[58] Y. F. Lyu,[39] F. C. Ma,[36] H. L. Ma,[1] L. L. Ma,[45] M. M. Ma,[1,58] Q. M. Ma,[1] R. Q. Ma,[1,58] R. T. Ma,[58] X. Y. Ma,[1,53] Y. Ma,[42,g] F. E. Maas,[17] M. Maggiora,[69a,69c] S. Maldaner,[4] S. Malde,[64] Q. A. Malik,[68] A. Mangoni,[26b] Y. J. Mao,[42,g] Z. P. Mao,[1] S. Marcello,[69a,69c] Z. X. Meng,[61] J. G. Messchendorp,[59,12] G. Mezzadri,[1,27a] H. Miao,[1] T. J. Min,[38] R. E. Mitchell,[25] X. H. Mo,[1,53,58] N. Yu. Muchnoi,[11,b] Y. Nefedov,[32] F. Nerling,[17,d] I. B. Nikolaev,[11] Z. Ning,[1,53] S. Nisar,[9,l] Y. Niu,[45] S. L. Olsen,[58] Q. Ouyang,[1,53,58] S. Pacetti,[26b,26c] X. Pan,[10,f] Y. Pan,[52] A. Pathak,[30] M. Pelizaeus,[4] H. P. Peng,[66,53] K. Peters,[12,d] J. Pettersson,[70] J. L. Ping,[37] R. G. Ping,[1,58] S. Plura,[31] S. Pogodin,[32] V. Prasad,[66,53] F. Z. Qi,[1] H. Qi,[66,53] H. R. Qi,[56] M. Qi,[38] T. Y. Qi,[10,f] S. Qian,[1,53] W. B. Qian,[58] Z. Qian,[54] C. F. Qiao,[58] J. J. Qin,[67] L. Q. Qin,[13] X. P. Qin,[10,f] X. S. Qin,[45] Z. H. Qin,[1,53] J. F. Qiu,[1] S. Q. Qu,[56] K. H. Rashid,[68] C. F. Redmer,[31] K. J. Ren,[35] A. Rivetti,[69c] V. Rodin,[59] M. Rolo,[69c] G. Rong,[1,58] Ch. Rosner,[17] S. N. Ruan,[39] H. S. Sang,[66] A. Sarantsev,[32,c] Y. Schelhaas,[31] C. Schnier,[4] K. Schönning,[70] M. Scodeggio,[27a,27b] K. Y. Shan,[10,f] W. Shan,[22] X. Y. Shan,[66,53] J. F. Shangguan,[50] L. G. Shao,[1,58] M. Shao,[66,53] C. P. Shen,[10,f] H. F. Shen,[1,58] X. Y. Shen,[1,58] B.-A. Shi,[58] H. C. Shi,[66,53] J. Y. Shi,[1] Q. Q. Shi,[50] R. S. Shi,[1,58] X. Shi,[1,53] X. D. Shi,[66,53] J. J. Song,[18] W. M. Song,[1,30] Y. X. Song,[42,g] S. Sosio,[69a,69c] S. Spataro,[69a,69c] F. Stieler,[31] K. X. Su,[71] P. P. Su,[50] Y.-J. Su,[58] G. X. Sun,[1] H. Sun,[58] H. K. Sun,[1] J. F. Sun,[18] L. Sun,[71] S. S. Sun,[1,58] T. Sun,[1,58] W. Y. Sun,[30] X. Sun,[23,h] Y. J. Sun,[66,53] Y. Z. Sun,[1] Z. T. Sun,[45] Y. H. Tan,[71] Y. X. Tan,[66,53] C. J. Tang,[49] G. Y. Tang,[1] J. Tang,[54] L. Y. Tao,[67] Q. T. Tao,[23,h] M. Tat,[64] J. X. Teng,[66,53] V. Thoren,[70] W. H. Tian,[47] Y. Tian,[28,58] I. Uman,[57b] B. Wang,[1] B. L. Wang,[58] C. W. Wang,[38] D. Y. Wang,[42,g] F. Wang,[67] H. J. Wang,[34,j,k] H. P. Wang,[1,58] K. Wang,[1,53] L. L. Wang,[1] M. Wang,[45] M. Z. Wang,[42,g] Meng Wang,[1,58] S. Wang,[10,f] T. Wang,[10,f] T. J. Wang,[39] W. Wang,[54] W. H. Wang,[71] W. P. Wang,[66,53] X. Wang,[42,g] X. F. Wang,[34,j,k] X. L. Wang,[10,f] Y. Wang,[56] Y. D. Wang,[41] Y. F. Wang,[1,53,58] Y. H. Wang,[43] Y. Q. Wang,[1] Yaqian Wang,[1,16] Z. Wang,[1,53] Z. Y. Wang,[1,58] Ziyi Wang,[58] D. H. Wei,[13] F. Weidner,[63] S. P. Wen,[1] D. J. White,[62] U. Wiedner,[4] G. Wilkinson,[64] M. Wolke,[70] L. Wollenberg,[4] J. F. Wu,[1,58] L. H. Wu,[1] L. J. Wu,[1,58] X. Wu,[10,f] X. H. Wu,[30] Y. Wu,[66] Z. Wu,[1,53] L. Xia,[66,53] T. Xiang,[42,g] D. Xiao,[34,j,k] G. Y. Xiao,[38] H. Xiao,[10,f]

S. Y. Xiao,[1] Y. L. Xiao,[10,f] Z. J. Xiao,[37] C. Xie,[38] X. H. Xie,[42,g] Y. Xie,[45] Y. G. Xie,[1,53] Y. H. Xie,[6] Z. P. Xie,[66,53] T. Y. Xing,[1,58] C. F. Xu,[1] C. J. Xu,[54] G. F. Xu,[1] H. Y. Xu,[61] Q. J. Xu,[15] S. Y. Xu,[65] X. P. Xu,[50] Y. C. Xu,[58] Z. P. Xu,[38] F. Yan,[10,f] L. Yan,[10,f] W. B. Yan,[66,53] W. C. Yan,[75] H. J. Yang,[46,e] H. L. Yang,[30] H. X. Yang,[1] L. Yang,[47] S. L. Yang,[58] Tao Yang,[1] Y. X. Yang,[1,58] Yifan Yang,[1,58] M. Ye,[1,53] M. H. Ye,[8] J. H. Yin,[1] Z. Y. You,[54] B. X. Yu,[1,53,58] C. X. Yu,[39] G. Yu,[1,58] T. Yu,[67] C. Z. Yuan,[1,58] L. Yuan,[2] S. C. Yuan,[1] X. Q. Yuan,[1] Y. Yuan,[1,58] Z. Y. Yuan,[54] C. X. Yue,[35] A. A. Zafar,[68] F. R. Zeng,[45] X. Zeng,[6] Y. Zeng,[23,h] Y. H. Zhan,[54] A. Q. Zhang,[1] B. L. Zhang,[1] B. X. Zhang,[1] D. H. Zhang,[39] G. Y. Zhang,[18] H. Zhang,[66] H. H. Zhang,[54] H. H. Zhang,[30] H. Y. Zhang,[1,53] J. L. Zhang,[72] J. Q. Zhang,[37] J. W. Zhang,[1,53,58] J. X. Zhang,[34,j,k] J. Y. Zhang,[1] J. Z. Zhang,[1,58] Jianyu Zhang,[1,58] Jiawei Zhang,[1,58] L. M. Zhang,[56] L. Q. Zhang,[54] Lei Zhang,[38] P. Zhang,[1] Q. Y. Zhang,[35,75] Shulei Zhang,[23,h] X. D. Zhang,[41] X. M. Zhang,[1] X. Y. Zhang,[45] X. Y. Zhang,[50] Y. Zhang,[64] Y. T. Zhang,[75] Y. H. Zhang,[1,53] Yan Zhang,[66,53] Yao Zhang,[1] Z. H. Zhang,[1] Z. Y. Zhang,[71] Z. Y. Zhang,[39] G. Zhao,[1] J. Zhao,[35] J. Y. Zhao,[1,58] J. Z. Zhao,[1,53] Lei Zhao,[66,53] Ling Zhao,[1] M. G. Zhao,[39] Q. Zhao,[1] S. J. Zhao,[75] Y. B. Zhao,[1,53] Y. X. Zhao,[28,58] Z. G. Zhao,[66,53] A. Zhemchugov,[32,a] B. Zheng,[67] J. P. Zheng,[1,53] Y. H. Zheng,[58] B. Zhong,[37] C. Zhong,[67] X. Zhong,[54] H. Zhou,[45] L. P. Zhou,[1,58] X. Zhou,[71] X. K. Zhou,[58] X. R. Zhou,[66,53] X. Y. Zhou,[35] Y. Z. Zhou,[10,f] J. Zhu,[39] K. Zhu,[1] K. J. Zhu,[1,53,58] L. X. Zhu,[58] S. H. Zhu,[65] S. Q. Zhu,[38] T. J. Zhu,[72] W. J. Zhu,[10,f] Y. C. Zhu,[66,53] Z. A. Zhu,[1,58] B. S. Zou,[1] and J. H. Zou[1]

(BESIII Collaboration)

[1]*Institute of High Energy Physics, Beijing 100049, People's Republic of China*
[2]*Beihang University, Beijing 100191, People's Republic of China*
[3]*Beijing Institute of Petrochemical Technology, Beijing 102617, People's Republic of China*
[4]*Bochum Ruhr-University, D-44780 Bochum, Germany*
[5]*Carnegie Mellon University, Pittsburgh, Pennsylvania 15213, USA*
[6]*Central China Normal University, Wuhan 430079, People's Republic of China*
[7]*Central South University, Changsha 410083, People's Republic of China*
[8]*China Center of Advanced Science and Technology, Beijing 100190, People's Republic of China*
[9]*COMSATS University Islamabad, Lahore Campus, Defence Road, Off Raiwind Road, 54000 Lahore, Pakistan*
[10]*Fudan University, Shanghai 200433, People's Republic of China*
[11]*G.I. Budker Institute of Nuclear Physics SB RAS (BINP), Novosibirsk 630090, Russia*
[12]*GSI Helmholtzcentre for Heavy Ion Research GmbH, D-64291 Darmstadt, Germany*
[13]*Guangxi Normal University, Guilin 541004, People's Republic of China*
[14]*Guangxi University, Nanning 530004, People's Republic of China*
[15]*Hangzhou Normal University, Hangzhou 310036, People's Republic of China*
[16]*Hebei University, Baoding 071002, People's Republic of China*
[17]*Helmholtz Institute Mainz, Staudinger Weg 18, D-55099 Mainz, Germany*
[18]*Henan Normal University, Xinxiang 453007, People's Republic of China*
[19]*Henan University of Science and Technology, Luoyang 471003, People's Republic of China*
[20]*Henan University of Technology, Zhengzhou 450001, People's Republic of China*
[21]*Huangshan College, Huangshan 245000, People's Republic of China*
[22]*Hunan Normal University, Changsha 410081, People's Republic of China*
[23]*Hunan University, Changsha 410082, People's Republic of China*
[24]*Indian Institute of Technology Madras, Chennai 600036, India*
[25]*Indiana University, Bloomington, Indiana 47405, USA*
[26a]*INFN Laboratori Nazionali di Frascati, INFN Laboratori Nazionali di Frascati, I-00044 Frascati, Italy*
[26b]*INFN Sezione di Perugia, I-06100 Perugia, Italy*
[26c]*University of Perugia, I-06100 Perugia, Italy*
[27a]*INFN Sezione di Ferrara, INFN Sezione di Ferrara, I-44122 Ferrara, Italy*
[27b]*University of Ferrara, I-44122 Ferrara, Italy*
[28]*Institute of Modern Physics, Lanzhou 730000, People's Republic of China*
[29]*Institute of Physics and Technology, Peace Ave. 54B, Ulaanbaatar 13330, Mongolia*
[30]*Jilin University, Changchun 130012, People's Republic of China*
[31]*Johannes Gutenberg University of Mainz, Johann-Joachim-Becher-Weg 45, D-55099 Mainz, Germany*
[32]*Joint Institute for Nuclear Research, 141980 Dubna, Moscow region, Russia*
[33]*Justus-Liebig-Universitaet Giessen, II. Physikalisches Institut, Heinrich-Buff-Ring 16, D-35392 Giessen, Germany*
[34]*Lanzhou University, Lanzhou 730000, People's Republic of China*
[35]*Liaoning Normal University, Dalian 116029, People's Republic of China*

[36]*Liaoning University, Shenyang 110036, People's Republic of China*
[37]*Nanjing Normal University, Nanjing 210023, People's Republic of China*
[38]*Nanjing University, Nanjing 210093, People's Republic of China*
[39]*Nankai University, Tianjin 300071, People's Republic of China*
[40]*National Centre for Nuclear Research, Warsaw 02-093, Poland*
[41]*North China Electric Power University, Beijing 102206, People's Republic of China*
[42]*Peking University, Beijing 100871, People's Republic of China*
[43]*Qufu Normal University, Qufu 273165, People's Republic of China*
[44]*Shandong Normal University, Jinan 250014, People's Republic of China*
[45]*Shandong University, Jinan 250100, People's Republic of China*
[46]*Shanghai Jiao Tong University, Shanghai 200240, People's Republic of China*
[47]*Shanxi Normal University, Linfen 041004, People's Republic of China*
[48]*Shanxi University, Taiyuan 030006, People's Republic of China*
[49]*Sichuan University, Chengdu 610064, People's Republic of China*
[50]*Soochow University, Suzhou 215006, People's Republic of China*
[51]*South China Normal University, Guangzhou 510006, People's Republic of China*
[52]*Southeast University, Nanjing 211100, People's Republic of China*
[53]*State Key Laboratory of Particle Detection and Electronics, Beijing 100049, Hefei 230026, People's Republic of China*
[54]*Sun Yat-Sen University, Guangzhou 510275, People's Republic of China*
[55]*Suranaree University of Technology, University Avenue 111, Nakhon Ratchasima 30000, Thailand*
[56]*Tsinghua University, Beijing 100084, People's Republic of China*
[57a]*Turkish Accelerator Center Particle Factory Group, Istinye University, 34010 Istanbul, Turkey*
[57b]*Near East University, Nicosia, North Cyprus, Mersin 10, Turkey*
[58]*University of Chinese Academy of Sciences, Beijing 100049, People's Republic of China*
[59]*University of Groningen, NL-9747 AA Groningen, The Netherlands*
[60]*University of Hawaii, Honolulu, Hawaii 96822, USA*
[61]*University of Jinan, Jinan 250022, People's Republic of China*
[62]*University of Manchester, Oxford Road, Manchester M13 9PL, United Kingdom*
[63]*University of Muenster, Wilhelm-Klemm-Str. 9, 48149 Muenster, Germany*
[64]*University of Oxford, Keble Rd, Oxford OX1 3RH, United Kingdom*
[65]*University of Science and Technology Liaoning, Anshan 114051, People's Republic of China*
[66]*University of Science and Technology of China, Hefei 230026, People's Republic of China*
[67]*University of South China, Hengyang 421001, People's Republic of China*
[68]*University of the Punjab, Lahore-54590, Pakistan*
[69a]*University of Turin and INFN, University of Turin, I-10125 Turin, Italy*
[69b]*University of Eastern Piedmont, I-15121 Alessandria, Italy*
[69c]*INFN, I-10125 Turin, Italy*
[70]*Uppsala University, Box 516, SE-75120 Uppsala, Sweden*
[71]*Wuhan University, Wuhan 430072, People's Republic of China*
[72]*Xinyang Normal University, Xinyang 464000, People's Republic of China*
[73]*Yunnan University, Kunming 650500, People's Republic of China*
[74]*Zhejiang University, Hangzhou 310027, People's Republic of China*
[75]*Zhengzhou University, Zhengzhou 450001, People's Republic of China*

[a]Also at the Moscow Institute of Physics and Technology, Moscow 141700, Russia.
[b]Also at the Novosibirsk State University, Novosibirsk 630090, Russia.
[c]Also at the NRC "Kurchatov Institute", PNPI, 188300 Gatchina, Russia.
[d]Also at Goethe University Frankfurt, 60323 Frankfurt am Main, Germany.
[e]Also at Key Laboratory for Particle Physics, Astrophysics and Cosmology, Ministry of Education; Shanghai Key Laboratory for Particle Physics and Cosmology; Institute of Nuclear and Particle Physics, Shanghai 200240, People's Republic of China.
[f]Also at Key Laboratory of Nuclear Physics and Ion-beam Application (MOE) and Institute of Modern Physics, Fudan University, Shanghai 200443, People's Republic of China.
[g]Also at State Key Laboratory of Nuclear Physics and Technology, Peking University, Beijing 100871, People's Republic of China.
[h]Also at School of Physics and Electronics, Hunan University, Changsha 410082, China.
[i]Also at Guangdong Provincial Key Laboratory of Nuclear Science, Institute of Quantum Matter, South China Normal University, Guangzhou 510006, China.
[j]Also at Frontiers Science Center for Rare Isotopes, Lanzhou University, Lanzhou 730000, People's Republic of China.
[k]Also at Lanzhou Center for Theoretical Physics, Lanzhou University, Lanzhou 730000, People's Republic of China.
[l]Also at the Department of Mathematical Sciences, IBA, Karachi, Pakistan.
[m]Also at Renmin University of China, Beijing 100872, People's Republic of China.

(Received 23 July 2022; accepted 29 November 2022; published 26 December 2022)

Using 4.5 fb^{-1} of e^+e^- annihilation data samples collected at the center-of-mass energies ranging from 4.600 GeV to 4.699 GeV with the BESIII detector at the BEPCII collider, a first study of the semileptonic decays $\Lambda_c^+ \to pK^-e^+\nu_e$, $\Lambda_c^+ \to \Lambda(1520)e^+\nu_e$ and $\Lambda_c^+ \to \Lambda(1405)e^+\nu_e$ is performed. The $\Lambda_c^+ \to pK^-e^+\nu_e$ decay is observed with a significance of 8.2σ and the branching fraction is measured to be $\mathcal{B}(\Lambda_c^+ \to pK^-e^+\nu_e) = (0.88 \pm 0.17_{\mathrm{stat}} \pm 0.07_{\mathrm{syst}}) \times 10^{-3}$. We also report evidence of $\Lambda_c^+ \to \Lambda(1520)e^+\nu_e$ and $\Lambda_c^+ \to \Lambda(1405)e^+\nu_e$ with significances of 3.3σ and 3.2σ, respectively, and measure $\mathcal{B}(\Lambda_c^+ \to \Lambda(1520)e^+\nu_e) = (1.02 \pm 0.52_{\mathrm{stat}} \pm 0.11_{\mathrm{syst}}) \times 10^{-3}$ and $\mathcal{B}(\Lambda_c^+ \to \Lambda(1405)[\to pK^-]e^+\nu_e) = (0.42 \pm 0.19_{\mathrm{stat}} \pm 0.04_{\mathrm{syst}}) \times 10^{-3}$. Combining these with the inclusive semileptonic Λ_c^+ branching fraction measured by BESIII, the relative fraction is determined to be $[\mathcal{B}(\Lambda_c^+ \to pK^-e^+\nu_e)/\mathcal{B}(\Lambda_c^+ \to Xe^+\nu_e)] = (2.1 \pm 0.4_{\mathrm{stat}} \pm 0.2_{\mathrm{syst}})\%$, which provides a clear confirmation that semileptonic Λ_c^+ decays are not saturated by the $\Lambda\ell^+\nu_\ell$ final state.

DOI: 10.1103/PhysRevD.106.112010

The study of Λ_c^+ semileptonic (SL) decays provides valuable informations about weak and strong interactions in baryons containing a heavy quark. (Throughout this paper, charge-conjugate modes are implied unless explicitly noted.) Their decay rates depend on the weak quark mixing Cabibbo-Kobayashi-Maskawa (CKM) matrix [1] element $|V_{cs}|$ and strong interaction effects parametrized by form factors describing the hadronic transition between the initial and the final baryons. In comparison to experimental studies of SL decays in the charmed meson sector [2], rather few measurements exist of Λ_c^+ SL decays. No other exclusive SL decay except $\Lambda_c^+ \to \Lambda\ell^+\nu_\ell$ ($\ell = e$, μ) has been reported to date [3,4]. In addition, a comparison of the branching fractions (BFs) for the exclusive decay $\Lambda_c^+ \to \Lambda\ell^+\nu_\ell$ and inclusive decay $\Lambda_c^+ \to X\ell^+\nu_\ell$ shows that their ratio is close to one [5], which exhibits a different pattern compared with charm mesons [2,6,7]. For example, the BF of $D^{+(0)} \to \bar{K}^0(K^-)e^+\nu_e$ is much smaller than $\mathcal{B}(D^{+(0)} \to e^+X)$ [2]. Searching for unknown exclusive SL Λ_c^+ decay can provide important information to validate and understand this pattern. The decay $\Lambda_c^+ \to pK^-e^+\nu_e$ is one of the best suited channels to search for [8–13], as its final state is simple with a high detection efficiency, in comparison to decays such as $\Lambda_c^+ \to \Sigma\pi e^+\nu_e$ etc.

Since the ud diquark is a spectator, the SL $\Lambda_c^+ \to pK^-e^+\nu_e$ decay provides a perfect filter of isospin $I = 0$ meson-baryon states with almost no contamination from the $I = 1$ amplitude [9,14]. This provides an ideal platform to study the internal structure of exotic Λ^* states. Among these states, particular interest is concentrated on the $\Lambda(1405)$, in which the high-mass pole strongly couples to $\bar{K}N$ final-state [2]. The $\Lambda(1405)$ is considered as the most striking state in understanding the spectrum of baryons with strangeness and has been continuously studied for more than 60 years since its theoretical prediction [15,16]. However, the nature of $\Lambda(1405)$ is still mysterious [17,18]. It is suggested to be a dynamically generated meson-baryon molecular state [9,16,19] or a three-quark uds bound state [8,10]. The decay of $\Lambda_c^+ \to \Lambda(1405)e^+\nu_e$ is expected to be a promising process to distinguish its structure because the predicted BF of the decay in the two hypotheses differ by a factor of roughly 100 times [8–10], as shown in Table I discussed later.

Furthermore, in heavy-baryon SL decays, most previous lattice quantum chromodynamics (LQCD) calculations are concentrated on the transition of $J^P = 1/2^+ \to J^P = 1/2^+$ [20–29], while the calculations regarding the transitions of $J^P = 1/2^+ \to J^P = 3/2^-$ are still very limited [30,31]. That is because the LQCD calculations in $1/2^+ \to 3/2^-$ are substantially more challenging due to the fact that the correlation functions for negative-parity baryons have more statistical noise than those for the lightest positive-parity baryons [32]. On the other hand, no experimental data is available to calibrate the calculations in $1/2^+ \to 3/2^-$ transitions [2]. Recently, LQCD extended the prediction on negative-parity baryons by performing the first calculation in $\Lambda_c^+ \to \Lambda(1520)\ell^+\nu_\ell$ [12,13] decays, under the approximation that the $\Lambda(1520)$ is a stable particle under the strong interaction because of its narrow width. An experimental measurement of $\Lambda_c^+ \to \Lambda(1520)e^+\nu_e$ will certainly provide a valuable check of the methodology applied in LQCD calculations, which is largely shared also with the calculations in Λ_b decays [13,30,31]. Comparison of the $\Lambda_c^+ \to \Lambda(1520)/\Lambda(1405)e^+\nu_e$ decay rates between measurement and theoretical predictions provides a necessary check of the calculations from the nonrelativistic quark model [10] and the constituent quark model [8].

In this paper, we perform the first study of the Λ_c^+ SL decay $\Lambda_c^+ \to pK^-e^+\nu_e$. We further search for SL decays of $\Lambda_c^+ \to \Lambda(1405)(\to pK^-)e^+\nu_e$ and $\Lambda_c^+ \to$

TABLE I. Comparison of $\mathcal{B}(\Lambda_c^+ \to \Lambda(1520)/\Lambda(1405)e^+\nu_e)$ [in $\times 10^{-3}$] between theoretical calculations and this measurement. The BF of $\Lambda(1405) \to pK^-$ is unknown [2].

	$\mathcal{B}(\Lambda_c^+ \to \Lambda(1520)e^+\nu_e)$	$\mathcal{B}(\Lambda_c^+ \to \Lambda(1405)e^+\nu_e)$
Constituent quark model [8]	1.01	3.04
Molecular state [9]	...	0.02
Nonrelativistic quark model [10]	0.60	2.43
Lattice QCD [12,13]	0.512 ± 0.082	...
Measurement	$1.02 \pm 0.52 \pm 0.11$	$\frac{0.42 \pm 0.19 \pm 0.04}{\mathcal{B}(\Lambda(1405) \to pK^-)}$

$\Lambda(1520)(\to pK^-)e^+\nu_e$, which are expected to represent the dominant components in $\Lambda_c^+ \to \Lambda^* e^+\nu_e$ decays [8,10], by investigating the pK^- invariant-mass spectrum in $\Lambda_c^+ \to pK^-e^+\nu_e$ data. The analysis is performed using data sets collected at BESIII with center-of-mass energies of $\sqrt{s} = 4.600$, 4.612, 4.628, 4.641, 4.661, 4.682, 4.699 GeV. The total integrated luminosity for these data sets is 4.5 fb^{-1} [33,34]. This is the largest data sample collected in e^+e^- collisions near the $\Lambda_c^+\bar{\Lambda}_c^-$ pair production threshold.

The construction and performance of the BESIII detector are described in detail in Ref. [35]. A GEANT4-based [36] Monte Carlo (MC) simulation package, which includes the geometric description of the detector and the detector response, is used to determine signal detection efficiencies and to estimate potential background contributions. Signal MC samples of $e^+e^- \to \Lambda_c^+\bar{\Lambda}_c^-$ with a Λ_c^+ baryon decaying to $pK^-e^+\nu_e$ or $\Lambda(1520)/\Lambda(1405)e^+\nu_e$ together with a $\bar{\Lambda}_c^-$ decaying to the analyzed hadronic decay mode described below are generated by KKMC [37] with EVTGEN [38], with initial-state radiation (ISR) [39] and final-state radiation (FSR) [40] effects included. The simulation of the SL decays $\Lambda_c^+ \to pK^-e^+\nu_e$ or $\Lambda_c^+ \to \Lambda(1405)/\Lambda(1520)e^+\nu_e$ is modeled with a phase-space generator. To study the possible peaking and combinatorial background contributions, inclusive MC samples consisting of open-charm states, radiative return to charmonium(-like) ψ states at lower masses and continuum processes of $q\bar{q}$ ($q = u, d, s$), along with Bhabha scattering, $\mu^+\mu^-$, $\tau^+\tau^-$ and $\gamma\gamma$ events are generated.

The first step of the analysis is the selection of "single-tag" (ST) events with a fully reconstructed $\bar{\Lambda}_c^-$ candidate. The $\bar{\Lambda}_c^-$ hadronic decay modes used in this analysis are $\bar{\Lambda}_c^- \to \bar{p}K_S^0$, $\bar{p}K^+\pi^-$, $\bar{p}K_S^0\pi^0$, $\bar{p}K^+\pi^-\pi^0$, $\bar{p}K_S^0\pi^+\pi^-$, $\bar{\Lambda}\pi^-$, $\bar{\Lambda}\pi^-\pi^0$, $\bar{\Lambda}\pi^-\pi^+\pi^-$, $\bar{\Sigma}^0\pi^-$, $\bar{\Sigma}^-\pi^0$, $\bar{\Sigma}^-\pi^+\pi^-$, $\bar{p}\pi^+\pi^-$, $\bar{\Sigma}^0\pi^+\pi^-\pi^-$, and $\bar{\Sigma}^0\pi^-\pi^0$, where the intermediate particles K_S^0, $\bar{\Lambda}$, $\bar{\Sigma}^0$, $\bar{\Sigma}^-$, and π^0 are reconstructed via their decays: $K_S^0 \to \pi^+\pi^-$, $\bar{\Lambda} \to \bar{p}\pi^+$, $\bar{\Sigma}^0 \to \gamma\bar{\Lambda}$ with $\bar{\Lambda} \to \bar{p}\pi^+$, $\bar{\Sigma}^- \to \bar{p}\pi^0$, and $\pi^0 \to \gamma\gamma$. Within this ST sample a search is then performed for $\Lambda_c^+ \to pK^-e^+\nu_e$ decay. The events passing this selection are referred to as the double-tag (DT) sample. For a specific tag mode i, the ST and DT event yields can be written as

$$N_{\mathrm{ST}}^i = 2N_{\bar{\Lambda}_c\Lambda_c}\mathcal{B}_{\mathrm{ST}}^i\epsilon_{\mathrm{ST}}^i \quad \text{and} \quad N_{\mathrm{DT}}^i = 2N_{\bar{\Lambda}_c\Lambda_c}\mathcal{B}_{\mathrm{ST}}^i\mathcal{B}_{\mathrm{SL}}\epsilon_{\mathrm{DT}}^i,$$

where $N_{\bar{\Lambda}_c\Lambda_c}$ is the number of $\bar{\Lambda}_c\Lambda_c$ pairs; $\mathcal{B}_{\mathrm{ST}}^i$ and $\mathcal{B}_{\mathrm{SL}}$ are the BFs of the $\bar{\Lambda}_c^-$ tag mode and the Λ_c^+ SL decay mode, respectively; ϵ_{ST}^i is the efficiency for finding the tag candidate; and ϵ_{DT}^i is the efficiency for simultaneously finding the tag $\bar{\Lambda}_c^-$ and the SL decay. The BF of the SL decay can be expressed as

$$\mathcal{B}_{\mathrm{SL}} = \frac{N_{\mathrm{DT}}}{\sum N_{\mathrm{ST}}^i \times \epsilon_{\mathrm{DT}}^i/\epsilon_{\mathrm{ST}}^i} = \frac{N_{\mathrm{DT}}}{N_{\mathrm{ST}} \times \epsilon_{\mathrm{SL}}}, \tag{1}$$

where N_{DT} is the total yield of DT events, N_{ST} is the total ST yield, and $\epsilon_{\mathrm{SL}} = \frac{\sum N_{\mathrm{ST}}^i \times \epsilon_{\mathrm{DT}}^i/\epsilon_{\mathrm{ST}}^i}{\sum N_{\mathrm{ST}}^i}$ is the average efficiency for finding a SL decay weighted by the relative yields of tag modes in data.

Selection criteria for γ, $\pi^\pm$, $K^\pm$, $p(\bar{p})$ as well as the reconstruction of π^0 and K_S^0 candidates are the same as those used in Refs. [3,4]. The invariant masses $M_{\bar{p}\pi^+}$, $M_{\gamma\bar{\Lambda}}$, and $M_{\bar{p}\pi^0}$ are required to be within $(1.110, 1.121)$ GeV$/c^2$, $(1.179, 1.205)$ GeV$/c^2$, and $(1.171, 1.204)$ GeV$/c^2$ to form candidates of $\bar{\Lambda}$, $\bar{\Sigma}^0$, and $\bar{\Sigma}^-$, respectively.

The ST $\bar{\Lambda}_c^-$ signals are identified using the beam-constrained mass,

$$M_{\mathrm{BC}} = \sqrt{(\sqrt{s}/2)^2/c^4 - |\vec{p}_{\bar{\Lambda}_c^-}|^2/c^2}, \tag{2}$$

where $\vec{p}_{\bar{\Lambda}_c^-}$ is the measured momentum of the ST $\bar{\Lambda}_c^-$. The energy difference $\Delta E = \sqrt{s}/2 - E_{\bar{\Lambda}_c^-}$ is defined to improve the signal significance for ST $\bar{\Lambda}_c^-$ baryons, where $E_{\bar{\Lambda}_c^-}$ is the measured energy. If more than one $\bar{\Lambda}_c^-$ tag is reconstructed in the event, only the tag with the minimum $|\Delta E|$ is kept to avoid double counting of STs with the same final state. The M_{BC} distributions at $\sqrt{s} = 4.682$ GeV for the fourteen ST modes are shown in Fig. 1. An unbinned maximum-likelihood fit is performed to the spectra, using the MC-simulated signal shape convolved with a Gaussian function accounting for differences of resolutions between data and MC simulation to describe the signal and an ARGUS function [41] to describe the background. The signal yield is determined in the mass region $(2.28, 2.30)$ GeV$/c^2$, which is regarded as the signal region. The ΔE requirements, the M_{BC} distributions for the other data sets and their ST yields are documented in the Appendix A.

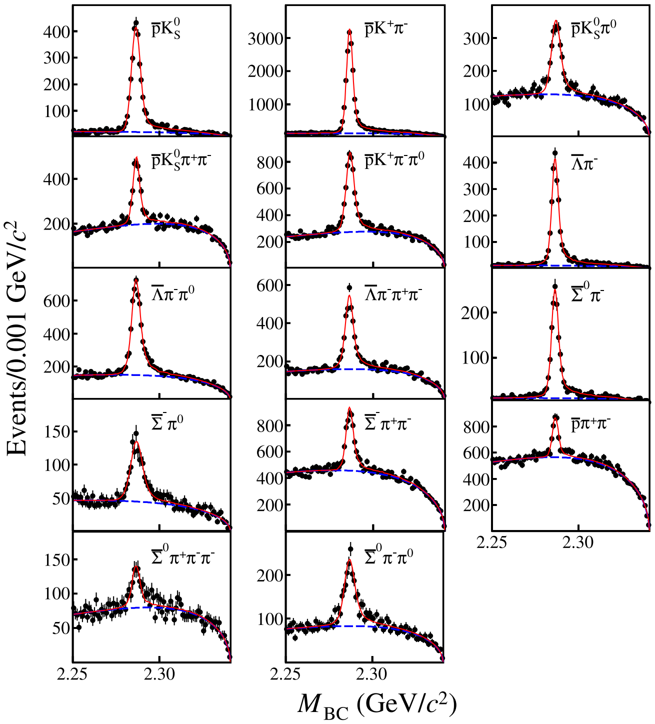

FIG. 1. Fits to the $M_{\rm BC}$ distributions for different ST modes at $\sqrt{s} = 4.682$ GeV. The points with error bars are data, the (red) solid curves show the total fits and the (blue) dashed curves are the fitted backgrounds.

The total ST yield reconstructed in the full data sample is $N_{\rm ST} = 122268 \pm 474$, where only the statistical uncertainty is reported.

Candidates from $\Lambda_c^+ \to pK^-e^+\nu_e$ are selected from the remaining particles recoiling against the ST $\bar{\Lambda}_c^-$ candidates, with the requirement that there be exactly three charged tracks. To select protons and kaons, the same criteria as those used in the ST selection are used. The proton and kaon charges must be opposite in sign. Detection and reconstruction of the positron follow the procedures in Ref. [3]. Background from $\Lambda_c^+ \to pK^-\pi^+$ decays is rejected by requiring the pK^-e^+ invariant mass ($M_{pK^-e^+}$) to be less than 2.15 GeV/c^2. To suppress contamination from $\Lambda_c^+ \to pK^-\pi^+\pi^0$ decays, a search is made for an additional π^0 in the recoiling system of the $\bar{\Lambda}_c^-$ baryon. If found, then a candidate $\Lambda_c^+ \to pK^-\pi^+\pi^0$ decay is reconstructed, where the positron is now assigned a pion hypothesis. For the event to be retained, it is required that the beam-constrained mass of this candidate falls outside the signal region.

The energy and momentum carried by the neutrino are denoted by $E_{\rm miss}$ and $\vec{p}_{\rm miss}$, respectively. They are calculated from the energies and momenta of the tag ($E_{\bar{\Lambda}_c^-}, \vec{p}_{\bar{\Lambda}_c^-}$) and the measured SL decay products ($E_{\rm SL} = E_p + E_{K^-} + E_{e^+}$, $\vec{p}_{\rm SL} = \vec{p}_p + \vec{p}_{K^-} + \vec{p}_{e^+}$) using the relations $E_{\rm miss} = \sqrt{s}/2 - E_{\rm SL}$ and $\vec{p}_{\rm miss} = \vec{p}_{\Lambda_c^+} - \vec{p}_{\rm SL}$ in the initial e^+e^- rest frame. Here, the momentum $\vec{p}_{\Lambda_c^+}$ is given by $\vec{p}_{\Lambda_c^+} = -\hat{p}_{\rm tag}\sqrt{(\sqrt{s}/2)^2 - m^2_{\bar{\Lambda}_c^-}}$, where $\hat{p}_{\rm tag}$ is the direction of the momentum of the ST $\bar{\Lambda}_c^-$ and $m_{\bar{\Lambda}_c^-}$ is the known $\bar{\Lambda}_c^-$ mass [2]. Information about the undetected neutrino is obtained by using the variable $U_{\rm miss}$,

$$U_{\rm miss} \equiv E_{\rm miss} - c|\vec{p}_{\rm miss}|. \tag{3}$$

The $U_{\rm miss}$ distribution is expected to peak at zero for the events of $\Lambda_c^+ \to pK^-e^+\nu_e$.

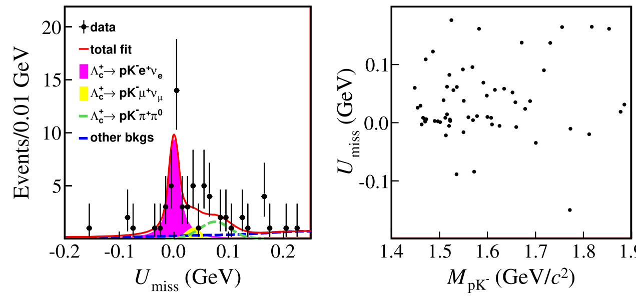

FIG. 2. (Left) Fit to the $U_{\rm miss}$ distribution for $\Lambda_c^+ \to pK^-e^+\nu_e$ in data. (Right) The distribution of $U_{\rm miss}$ *vs.* M_{pK^-} for $\Lambda_c^+ \to pK^-e^+\nu_e$ candidates.

Figure 2 (left) shows the $U_{\rm miss}$ distribution of the reconstructed candidates for $\Lambda_c^+ \to pK^-e^+\nu_e$ in data. To obtain the signal yield, the $U_{\rm miss}$ distribution is described with four components: a signal function f which consists of a Gaussian to describe the core of the $U_{\rm miss}$ distribution and two power-law tails to account for initial- and final-state radiation [3,42], two MC-derived shapes describing components from $\Lambda_c^+ \to pK^-\pi^+\pi^0$ and $\Lambda_c^+ \to pK^-\mu^+\nu_\mu$, and an MC-derived nonresonant shape describing the combinatorial backgrounds. The yield of the $\Lambda_c^+ \to pK^-\mu^+\nu_\mu$ component, $N_{\rm DT}^{pK^-\mu^+\nu_\mu}$, is related to $N_{\rm DT}^{pK^-e^+\nu_e}$, which is the yield of $\Lambda_c^+ \to pK^-e^+\nu_e$ decay, by

$$N_{\rm DT}^{pK^-\mu^+\nu_\mu} = N_{\rm DT}^{pK^-e^+\nu_e} \times R_\epsilon \times R_{\mathcal{B}}, \tag{4}$$

where $R_{\mathcal{B}} = \frac{\mathcal{B}(\Lambda_c^+ \to pK^-\mu^+\nu_\mu)}{\mathcal{B}(\Lambda_c^+ \to pK^-e^+\nu_e)} = 0.88 \pm 0.03$ [10]. The uncertainty on $R_{\mathcal{B}}$ is evaluated by comparing the difference of the BFs of $\Lambda(1405)$ and $\Lambda(1520)$ resonances decaying into $N\bar{K}e^+\nu_e$ and $N\bar{K}\mu^+\nu_\mu$ final states. The parameter R_ϵ, defined as the relative detection efficiency between $\Lambda_c^+ \to pK^-\mu^+\nu_\mu$ and $\Lambda_c^+ \to pK^-e^+\nu_e$, is evaluated to be 0.15 with MC simulation. The event yield for $\Lambda_c^+ \to pK^-e^+\nu_e$, as determined from the fit to the $U_{\rm miss}$ distribution, is $N_{\rm DT}^{pK^-e^+\nu_e} = 33.5 \pm 6.3$, where the uncertainty is statistical. The statistical significance of the $\Lambda_c^+ \to pK^-e^+\nu_e$ signal is determined to be 8.9σ, calculated via $\sqrt{-2 \times \Delta \ln \mathcal{L}}$, where $\Delta \ln \mathcal{L}$ is the variation in $\ln \mathcal{L}$ of the likelihood fit with and without the signal component included.

To search for $\Lambda_c^+ \to \Lambda(1520)/\Lambda(1405)e^+\nu_e$, the distribution of $U_{\rm miss}$ *vs.* M_{pK^-} is studied, as shown in Fig. 2 (right). An accumulation of events around the intersection of the $\Lambda(1520)/\Lambda(1405)$ and $pK^-e^+\nu_e$ signal regions is observed. To extract the yield of $\Lambda_c^+ \to \Lambda(1520)/\Lambda(1405)e^+\nu_e$, a two-dimensional (2D) likelihood fit is performed to the M_{pK^-} and $U_{\rm miss}$ distributions. For each component, the 2D distribution of M_{pK^-} and $U_{\rm miss}$ is modeled with a product of two one-dimensional probability density functions (PDFs), one for each dimension. The signal functions in the M_{pK^-} distribution for $\Lambda(1520)$ and $\Lambda(1405)$ are described by a Breit-Wigner (BW) function and a Flatté-parametrization [43], respectively. The masses and widths for $\Lambda(1520)$ and $\Lambda(1405)$ are fixed to the PDG values [2]. The M_{pK^-} distributions of the nonresonant (NR) components of $\Lambda_c^+ \to (pK^-)_{\rm NR}e^+\nu_e$ and $\Lambda_c^+ \to pK^-\mu^+\nu_\mu$ are described with phase-space models, while for the components from $\Lambda_c^+ \to pK^-\pi^+\pi^0$ and the other background sources, the MC-derived shapes are used to describe the M_{pK^-} distributions. The $U_{\rm miss}$ distributions from $\Lambda_c^+ \to \Lambda(1520/1405)e^+\nu_e$ and $\Lambda_c^+ \to (pK^-)_{\rm NR}e^+\nu_e$ decays are both described by the function f with parameters taken from MC simulation. For the other components, the shapes obtained from MC simulation are used. The projection of the 2D fit on the M_{pK^-} axis is shown in Fig. 3. The fitted DT yields for $\Lambda_c^+ \to \Lambda(1520)e^+\nu_e$ and $\Lambda_c^+ \to \Lambda(1405)e^+\nu_e$ are 8.4 ± 4.3 and 14.8 ± 6.7, respectively, where the uncertainties are statistical only. The statistical significance of including only $\Lambda_c^+ \to \Lambda(1520)e^+\nu_e$ or $\Lambda_c^+ \to \Lambda(1405)e^+\nu_e$ is evaluated to be 3.8σ for both, with respect to the hypothesis that neither of the two states is included. It suggests that the two resonances contribute equally and neither of them can be neglected.

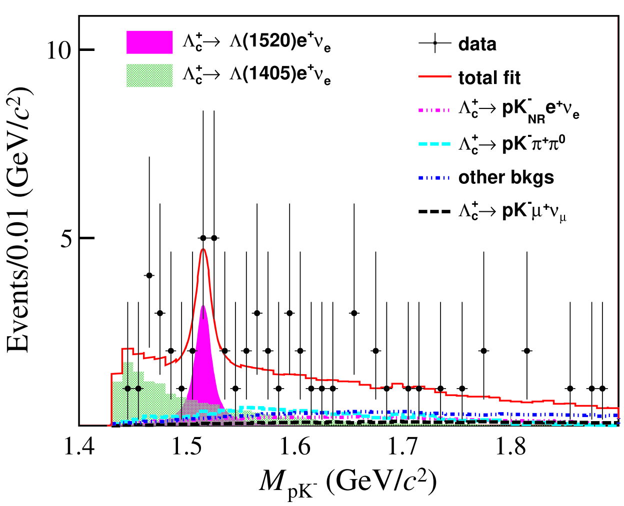

FIG. 3. Projection of the 2D-fit on the M_{pK^-} axis for $\Lambda_c^+ \to pK^-e^+\nu_e$ candidates in data.

The averaged efficiencies for detecting the $\Lambda_c^+ \to pK^-e^+\nu_e$, $\Lambda_c^+ \to \Lambda(1520)(\to pK^-)e^+\nu_e$ and $\Lambda_c^+ \to \Lambda(1405)(\to pK^-)e^+\nu_e$ decays are determined to be $\epsilon_{\rm SL}^{pK^-e^+\nu_e} = (31.01 \pm 0.31)\%$, $\epsilon_{\rm SL}^{\Lambda(1520)(\to pK^-)e^+\nu_e} = (30.03 \pm 0.31)\%$ and $\epsilon_{\rm SL}^{\Lambda(1405)(\to pK^-)e^+\nu_e} = (28.64 \pm 0.32)\%$, respectively. Inserting the values of their DT yields, averaged efficiencies and $N^{\rm ST}$ into Eq. (1), results in $\mathcal{B}(\Lambda_c^+ \to pK^-e^+\nu_e) = (0.88 \pm 0.17 \pm 0.07) \times 10^{-3}$, $\mathcal{B}(\Lambda_c^+ \to \Lambda(1520)[\to pK^-]e^+\nu_e) = (0.23 \pm 0.12 \pm 0.02) \times 10^{-3}$ and $\mathcal{B}(\Lambda_c^+ \to \Lambda(1405)[\to pK^-]e^+\nu_e) = (0.42 \pm 0.19 \pm 0.04) \times 10^{-3}$, where the first uncertainties are statistical and the second are systematic. Due to limited data, the possible interference effects between $\Lambda_c^+ \to \Lambda(1520/1405)e^+\nu_e$ and $\Lambda_c^+ \to (pK^-)_{\rm NR}e^+\nu_e$, as well as interference between $\Lambda(1520)$ and $\Lambda(1405)$ states, are ignored.

The DT technique means that the measured BFs are insensitive to any systematic uncertainties in the ST selection, as the effects of the ST selection criteria are canceled for both data and MC in the determination of the BFs. Sources of systematic uncertainty are, instead, related to the tracking and PID efficiencies of the e^+ (0.4% and 0.5%, respectively), p (1% and 1%), and K^- (1% and 1%), evaluated with control samples of radiative Bhabha scattering, $J/\psi \to p\bar{p}\pi^+\pi^-$ and $J/\psi \to K_S^0K^\mp\pi^\pm$ events, respectively. The uncertainties arising from the fit are determined by using alternative line shapes to parametrize the signal and background contributions. For $\Lambda_c^+ \to pK^-e^+\nu_e$, the alternative fit uses the shape from MC simulation for the signal, with a constant to describe the combinatorial background for the $U_{\rm miss}$ distribution, which results in an uncertainty of 3.8%. For $\Lambda_c^+ \to \Lambda(1520)/\Lambda(1405)e^+\nu_e$, the masses and widths of the signal-function are varied by $\pm 1\sigma$, and a data-driven M_{pK^-} shape is used to describe the $\Lambda_c^+ \to pK^-\pi^+\pi^0$ background, which results in an uncertainty of 4.6/3.9%. The uncertainties due to the knowledge of $R_{\mathcal{B}}$ on the three BFs are estimated to be 3.0%, 1.4%, and 1.4% by varying the nominal value of $R_{\mathcal{B}}$ by ± 0.03 in the fits. The uncertainty of neglecting the possible decay $\Lambda_c^+ \to \Lambda(1520/1405)(\to pK^-)\mu^+\nu_\mu$ is evaluated to be 4.8/5.4%, by varying the description of $\Lambda_c^+ \to pK^-\mu^+\nu_\mu$ component with $\Lambda_c^+ \to (pK^-)_{\rm NR}\mu^+\nu_\mu$ and $\Lambda_c^+ \to \Lambda(1520)/\Lambda(1405)\mu^+\nu_\mu$. The uncertainty arising from the MC model of $\Lambda_c^+ \to pK^-e^+\nu_e$ is assigned by varying the relative fraction of $\Lambda_c^+ \to (pK^-)_{\rm NR}e^+\nu_e$ and $\Lambda_c^+ \to \Lambda(1520)/\Lambda(1405)e^+\nu_e$ by $\pm 1\sigma$ in the MC generation. In the case of $\Lambda_c^+ \to \Lambda(1520)/\Lambda(1405)e^+\nu_e$, a new MC model based on leading-order heavy-quark effective theory is introduced [10]. These alternative models lead to a relative difference of 3.7% and 2.7/3.6% in the efficiencies of $\Lambda_c^+ \to pK^-e^+\nu_e$ and $\Lambda_c^+ \to \Lambda(1520)/\Lambda(1405)e^+\nu_e$, respectively, which is assigned as the corresponding uncertainty. To account for neglecting possible interference effects in measuring the BF of $\Lambda_c^+ \to \Lambda(1520)/\Lambda(1405)e^+\nu_e$, an additional 6.1% uncertainty is assigned based on studies of the inclusive $K\pi$ system in D SL decays [44,45]. In addition the uncertainties of the requirements on $M_{\rm BC}$ (2.1%), $M_{pK^-e^+}$ (3.1%), $N_{\rm ST}$ (1.0%) and the MC sample size (1.0%) are considered. Adding these contributions in quadrature gives a total systematic uncertainty of 7.8% for $\mathcal{B}(\Lambda_c^+ \to pK^-e^+\nu_e)$, 10.4% for $\mathcal{B}(\Lambda_c^+ \to \Lambda(1520)e^+\nu_e)$ and 10.7% for $\mathcal{B}(\Lambda_c^+ \to \Lambda(1405)e^+\nu_e)$. When considering each of these systematic contributions in turn, the minimum significance for $\Lambda_c^+ \to pK^-e^+\nu_e$ is determined to be 8.2σ. The minimum significance for $\Lambda_c^+ \to \Lambda(1520)e^+\nu_e$ and $\Lambda_c^+ \to \Lambda(1405)e^+\nu_e$ are determined to be 3.3σ and 3.2σ, respectively.

In summary, using 4.5 fb^{-1} of data collected at the center-of-mass energies from 4.600 GeV to 4.699 GeV, the SL decay $\Lambda_c^+ \to pK^-e^+\nu_e$ is observed with 8.2σ significance. We also find evidence for $\Lambda_c^+ \to \Lambda(1520)e^+\nu_e$ and $\Lambda_c^+ \to \Lambda(1405)e^+\nu_e$ with a significance of 3.3σ and 3.2σ, respectively. The measured BFs are $\mathcal{B}(\Lambda_c^+ \to pK^-e^+\nu_e) = (0.88 \pm 0.17 \pm 0.07) \times 10^{-3}$, $\mathcal{B}(\Lambda_c^+ \to \Lambda(1520)[\to pK^-]e^+\nu_e) = (0.23 \pm 0.12 \pm 0.02) \times 10^{-3}$ and $\mathcal{B}(\Lambda_c^+ \to \Lambda(1405)[\to pK^-]e^+\nu_e) = (0.42 \pm 0.19 \pm 0.04) \times 10^{-3}$. Taking into account that $\mathcal{B}(\Lambda(1520) \to N\bar{K}) = (45 \pm 1)\%$ [2], we measure $\mathcal{B}(\Lambda_c^+ \to \Lambda(1520)e^+\nu_e) = (1.02 \pm 0.52 \pm 0.11) \times 10^{-3}$. Comparisons of $\mathcal{B}(\Lambda_c^+ \to \Lambda(1520)/\Lambda(1405)e^+\nu_e)$ between the measurement and predicted values from theoretical models [8–10] as well as the LQCD [12,13] are shown in Table I. Our measured $\mathcal{B}(\Lambda_c^+ \to \Lambda(1520)e^+\nu_e)$ is consistent with these theoretical calculations within two standard deviations.

Combing the BF of $\Lambda_c^+ \to \Lambda(1520)e^+\nu_e$ measured in this work, τ_{Λ_c} and the q^2-integrated rate predicted by LQCD [12,13], we determine $|V_{cs}| = 1.3 \pm 0.3_{\mathcal{B}} \pm 0.1_{\rm LQCD}$, which is in consistent with $|V_{cs}| = 0.97401(11)$ obtained assuming CKM unitarity [2] within one standard deviation. This is the first determination of $|V_{cs}|$ using data of baryonic SL decays in excited Λ state. Our results presented in this paper are valuable in extending the understanding of Λ_c^+ SL decays beyond the mode $\Lambda_c^+ \to \Lambda\ell^+\nu_\ell$, and represent a significant advance in knowledge since the discovery of the Λ_c^+ more than 40 years ago. The observation of $\Lambda_c^+ \to pK^-e^+\nu_e$ is that of the first SL Λ_c decay mode that does not contain a Λ baryon in the final state [8,11]. In addition, the observed pK^- invariant-mass spectrum in this work can provide new insights into the internal structure of excited Λ states as well as in the study of hyperon spectroscopy [9,14,17,46,47], complementary to the informations from the pentaquark searches using $\Lambda_b \to pK^-J/\psi$ [43]. With the larger samples that BESIII expects to collect [48], an amplitude analysis of the pK^- mass spectrum will be performed to understand the internal structure of the contributing Λ^* states.

The BESIII Collaboration thanks the staff of BEPCII and the IHEP computing center for their strong support. This work is supported in part by National Key R&D Program of China under Contracts No. 2020YFA0406400, and No. 2020YFA0406300; National Natural Science Foundation of China (NSFC) under Contracts No. 11635010, No. 11735014, No. 11835012, No. 11935015, No. 11935016, No. 11935018, No. 11961141012, No. 12022510, No. 12025502, No. 12035009, No. 12035013, No. 12192260, No. 12192261, No. 12192262, No. 12192263, No. 12192264, and No. 12192265; the Chinese Academy of Sciences (CAS) Large-Scale Scientific Facility Program; Joint Large-Scale Scientific Facility Funds of the NSFC and CAS under Contract No. U1832207; CAS Key Research Program of Frontier Sciences under Contract No. QYZDJ-SSW-SLH040; 100 Talents Program of CAS; INPAC and Shanghai Key Laboratory for Particle Physics and Cosmology; ERC under Contract No. 758462; European Union's Horizon 2020 research and innovation programme under Marie Sklodowska-Curie grant agreement under Contract No. 894790; German Research Foundation DFG under Contracts Nos. 443159800, Collaborative Research Center CRC 1044, GRK 2149; Istituto Nazionale di Fisica Nucleare, Italy; Ministry of Development of Turkey under Contract No. DPT2006K-120470; National Science and Technology fund; STFC (United Kingdom); The Royal Society, UK under Contracts No. DH140054 and No. DH160214; The Swedish Research Council; U.S. Department of Energy under Contract No. DE-FG02-05ER41374.

APPENDIX: THE $M_{\rm BC}$ DISTRIBUTIONS FOR THE OTHER DATA SETS

Figures 4, 5, and 6 show the $M_{\rm BC}$ distributions obtained at $\sqrt{s} = 4.600$, 4.612, 4.628, 4.641, 4.661, and 4.699 GeV, respectively. The ST yields for each of the ST modes collected at different energy points are given in Table II.

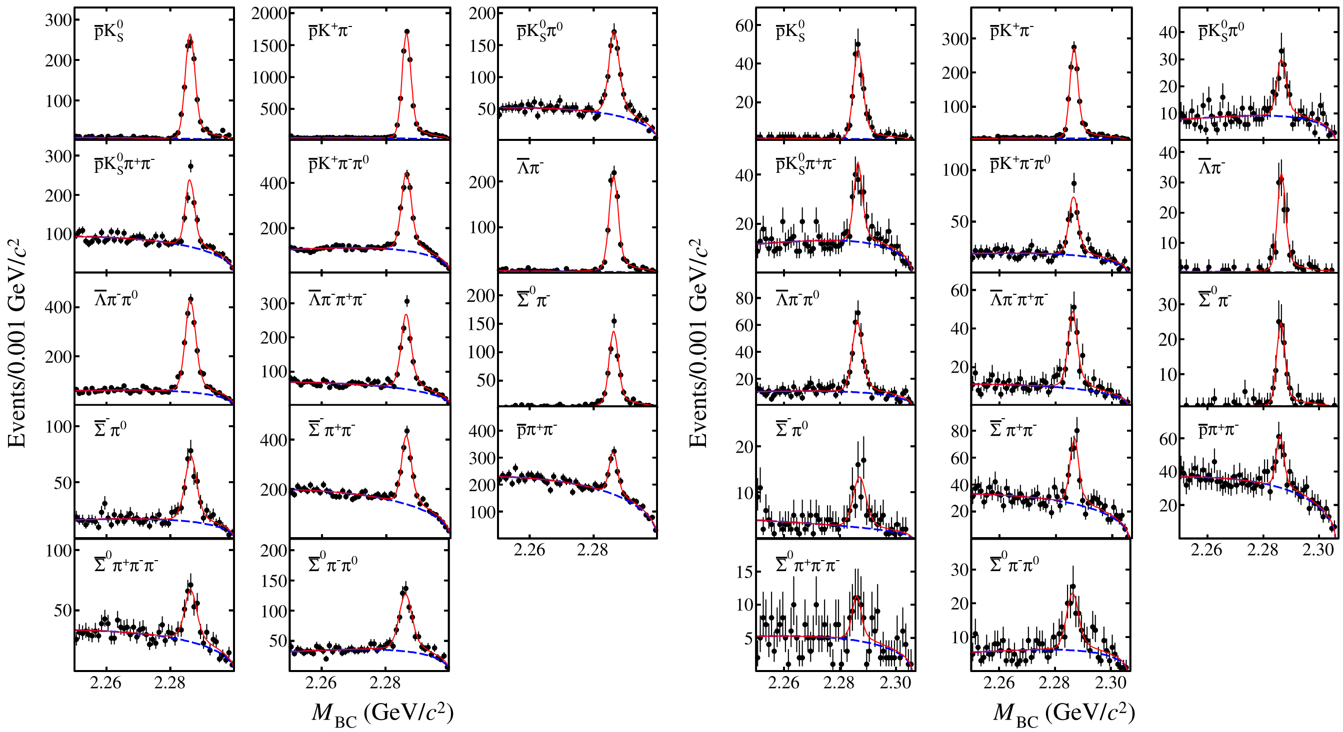

FIG. 4. Fits to M_{BC} distributions for different ST modes at (left) $\sqrt{s} = 4.600$ GeV and (right) $\sqrt{s} = 4.612$ GeV. The points with error bars are data, the (red) solid curves show the total fits and the (blue) dashed curves are the background shapes.

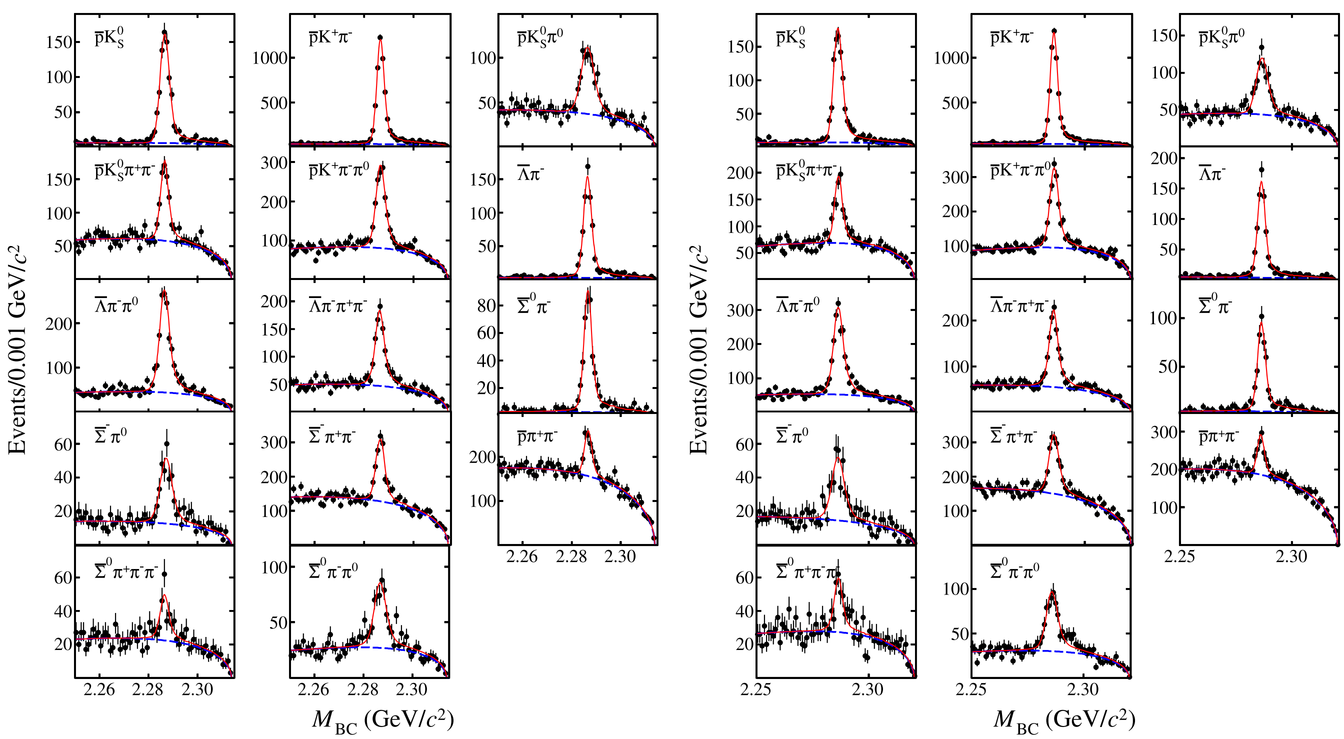

FIG. 5. Fits to M_{BC} distributions for different ST modes at (left) $\sqrt{s} = 4.628$ GeV and (right) $\sqrt{s} = 4.641$ GeV. The points with error bars are data, the (red) solid curves show the total fits and the (blue) dashed curves are the background shapes.

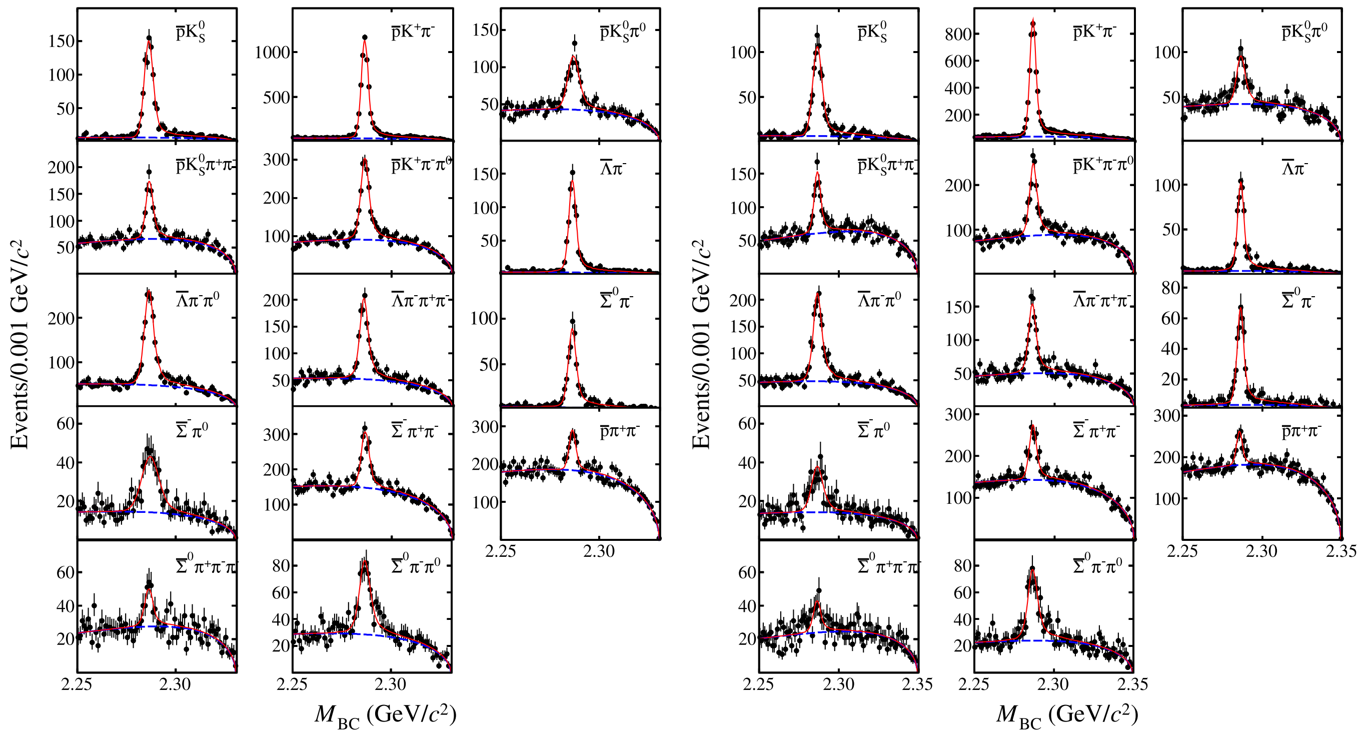

FIG. 6. Fits to $M_{\rm BC}$ distributions for different ST modes at (left) $\sqrt{s} = 4.661$ GeV and (right) $\sqrt{s} = 4.699$ GeV. The points with error bars are data, the (red) solid curves show the total fits and the (blue) dashed curves are the background shapes.

TABLE II. The ΔE requirements and the ST yields $N_{\rm ST}$ in each of the data sets.

$\bar{\Lambda}_c^- \to$	ΔE (GeV)	$N_{\rm ST}^{4600}$	$N_{\rm ST}^{4612}$	$N_{\rm ST}^{4628}$	$N_{\rm ST}^{4641}$	$N_{\rm ST}^{4661}$	$N_{\rm ST}^{4682}$	$N_{\rm ST}^{4699}$
$\bar{p}K_S^0$	$[-0.031, 0.033]$	1144 ± 38	230 ± 17	837 ± 34	948 ± 35	922 ± 34	2816 ± 59	791 ± 31
$\bar{p}K^+\pi^-$	$[-0.030, 0.039]$	6692 ± 90	1123 ± 37	5174 ± 81	5935 ± 86	5572 ± 82	16512 ± 139	4834 ± 75
$\bar{p}K_S^0\pi^0$	$[-0.049, 0.052]$	622 ± 42	103 ± 15	545 ± 40	550 ± 41	568 ± 40	1649 ± 62	411 ± 34
$\bar{p}K_S^0\pi^+\pi^-$	$[-0.048, 0.049]$	729 ± 41	145 ± 18	566 ± 36	644 ± 40	585 ± 38	1738 ± 66	555 ± 38
$\bar{p}K^+\pi^-\pi^0$	$[-0.043, 0.051]$	1598 ± 62	275 ± 24	1163 ± 54	1319 ± 62	1295 ± 55	3943 ± 97	1077 ± 50
$\bar{\Lambda}\pi^-$	$[-0.031, 0.034]$	878 ± 30	143 ± 12	712 ± 30	792 ± 29	730 ± 29	2254 ± 50	580 ± 26
$\bar{\Lambda}\pi^-\pi^0$	$[-0.044, 0.057]$	1803 ± 56	279 ± 22	1339 ± 48	1600 ± 52	1443 ± 49	4211 ± 85	1258 ± 47
$\bar{\Lambda}\pi^-\pi^+\pi^-$	$[-0.043, 0.045]$	1023 ± 44	199 ± 18	737 ± 39	960 ± 44	935 ± 43	2599 ± 77	710 ± 39
$\bar{\Sigma}^0\pi^-$	$[-0.032, 0.040]$	577 ± 28	105 ± 11	424 ± 24	467 ± 25	503 ± 24	1423 ± 41	384 ± 21
$\bar{\Sigma}^-\pi^0$	$[-0.050, 0.060]$	310 ± 25	70 ± 11	264 ± 23	282 ± 26	314 ± 26	827 ± 42	222 ± 23
$\bar{\Sigma}^-\pi^+\pi^-$	$[-0.043, 0.052]$	1234 ± 62	224 ± 24	942 ± 51	1069 ± 64	938 ± 53	2941 ± 96	858 ± 54
$\bar{p}^-\pi^+\pi^-$	$[-0.040, 0.040]$	603 ± 48	128 ± 21	454 ± 45	490 ± 48	528 ± 49	1553 ± 86	443 ± 50
$\bar{\Sigma}^0\pi^+\pi^-\pi^-$	$[-0.030, 0.030]$	224 ± 18	34 ± 10	150 ± 22	185 ± 24	144 ± 23	420 ± 40	133 ± 23
$\bar{\Sigma}^0\pi^-\pi^0$	$[-0.030, 0.032]$	541 ± 36	102 ± 15	392 ± 30	470 ± 32	418 ± 31	1246 ± 53	437 ± 30

[1] M. Kobayashi and T. Maskawa, Prog. Theor. Phys. **49**, 652 (1973).
[2] P. A. Zyla *et al.* (Particle Data Group), Prog. Theor. Exp. Phys. **2020**, 083C01 (2020) and 2021 update.
[3] M. Ablikim *et al.* (BESIII Collaboration), Phys. Rev. Lett. **115**, 221805 (2015).
[4] M. Ablikim *et al.* (BESIII Collaboration), Phys. Lett. B **767**, 42 (2017).
[5] M. Ablikim *et al.* (BESIII Collaboration), Phys. Rev. Lett. **121**, 251801 (2018).
[6] Q. A. Zhang, H. Hua, F. Huang, R. Li, Y. Li, C. D. Lü, P. Sun, W. Wang, and Y. B. Yang, Chin. Phys. C **46**, 011002 (2022).
[7] Y. S. Li, X. Liu, and F. S. Yu, Phys. Rev. D **104**, 013005 (2021).
[8] M. Pervin, W. Roberts, and S. Capstick, Phys. Rev. C **72**, 035201 (2005).
[9] N. Ikeno and E. Oset, Phys. Rev. D **93**, 014021 (2016).
[10] M. M. Hussain and W. Roberts, Phys. Rev. D **95**, 053005 (2017); **95**, 099901(E) (2017).
[11] M. Gronau and J. L. Rosner, Phys. Rev. D **97**, 116015 (2018).
[12] S. Meinel and G. Rendon, Phys. Rev. D **105**, L051505 (2022).
[13] S. Meinel and G. Rendon, Phys. Rev. D **105**, 054511 (2022).
[14] K. Miyahara, T. Hyodo, and E. Oset, Phys. Rev. C **92**, 055204 (2015).
[15] R. H. Dalitz and S. F. Tuan, Phys. Rev. Lett. **2**, 425 (1959).
[16] R. H. Dalitz and S. F. Tuan, Ann. Phys. (N.Y.) **10**, 307 (1960).
[17] T. Hyodo and M. Niiyama, Prog. Part. Nucl. Phys. **120**, 103868 (2021).
[18] M. Mai, Eur. Phys. J. Spec. Top. **230**, 1593 (2021).
[19] R. H. Dalitz, T. C. Wong, and G. Rajasekaran, Phys. Rev. **153**, 1617 (1967).
[20] K. C. Bowler, R. D. Kenway, L. Lellouch, J. Nieves, O. Oliveira, D. G. Richards, C. T. Sachrajda, N. Stella, and P. Ueberholz, Phys. Rev. D **57**, 6948 (1998).
[21] S. Gottlieb and S. Tamhankar, Nucl. Phys. B, Proc. Suppl. **119**, 644 (2003).
[22] A. Datta, S. Kamali, S. Meinel, and A. Rashed, J. High Energy Phys. 08 (2017) 131.
[23] W. Detmold, C. Lehner, and S. Meinel, Phys. Rev. D **92**, 034503 (2015).
[24] W. Detmold, C.-J. David Lin, S. Meinel, and M. Wingate, Phys. Rev. D **88**, 014512 (2013).
[25] W. Detmold, C.-J. David Lin, S. Meinel, and M. Wingate, Phys. Rev. D **87**, 074502 (2013).
[26] W. Detmold and S. Meinel, Phys. Rev. D **93**, 074501 (2016).
[27] S. Meinel, Phys. Rev. Lett. **118**, 082001 (2017).
[28] S. Meinel, Phys. Rev. D **97**, 034511 (2018).
[29] Q. A. Zhang, H. Hua, F. Huang, R. Li, Y. Li, C. D. Lü, P. Sun, W. Wang, and Y. B. Yang, Chin. Phys. C **46**, 011002 (2022).
[30] S. Meinel and G. Rendon, Phys. Rev. D **103**, 074505 (2021).
[31] S. Meinel and G. Rendon, Phys. Rev. D **103**, 094516 (2021).
[32] P. A. Boyle *et al.*, arXiv:2205.15373.
[33] M. Ablikim *et al.* (BESIII Collaboration), Chin. Phys. C **39**, 093001 (2015).
[34] M. Ablikim *et al.* (BESIII Collaboration), Chin. Phys. C **46**, 113003 (2022).
[35] M. Ablikim *et al.* (BESIII Collaboration), Nucl. Instrum. Methods Phys. Res., Sect. A **614**, 345 (2010).
[36] S. Agostinelli *et al.* (GEANT4 Collaboration), Nucl. Instrum. Methods Phys. Res., Sect. A **506**, 250 (2003).
[37] S. Jadach, B. F. L. Ward, and Z. Was, Comput. Phys. Commun. **130**, 260 (2000); Phys. Rev. D **63**, 113009 (2001).
[38] D. J. Lange, Nucl. Instrum. Methods Phys. Res., Sect. A **462**, 152 (2001); R. G. Ping, Chin. Phys. C **32**, 599 (2008).
[39] E. A. Kurav and V. S. Fadin, Sov. J. Nucl. Phys. **41**, 466 (1985).
[40] E. Richter-Was, Phys. Lett. B **303**, 163 (1993).
[41] H. Albrecht *et al.* (ARGUS Collaboration), Phys. Lett. B **241**, 278 (1990).
[42] J. Y. Ge *et al.* (CLEO Collaboration), Phys. Rev. D **79**, 052010 (2009).
[43] R. Aaij *et al.* (LHCb Collaboration), Phys. Rev. Lett. **115**, 072001 (2015).
[44] M. Ablikim *et al.* (BESIII Collaboration), Phys. Rev. D **94**, 032001 (2016).
[45] M. Ablikim *et al.* (BESIII Collaboration), Phys. Rev. D **99**, 011103R (2019).
[46] T. Hyodo and D. Jido, Prog. Part. Nucl. Phys. **67**, 55 (2012).
[47] L. Roca, M. Mai, E. Oset, and Ulf-G. Meißner, Eur. Phys. J. C **75**, 218 (2015).
[48] M. Ablikim *et al.* (BESIII Collaboration), Chin. Phys. C **44**, 040001 (2020).